EUROPEAN ORGANIZATION FOR NUCLEAR RESEARCH

Proposal to the ISOLDE and Neutron Time-of-Flight Committee

Probing Energy Efficient Perovskites

September 22, 2020

A.M.L. Lopes[1], J. Schell[2,6], V.S. Amaral[3], J.P. Araujo[1], A. Burimova[4], A. W. Carbonari[4], E. L. Correa[11], J.G. Correia[5, 6], T. T. Dang[2], M. Escobar[2], R. S. Freitas[13], A.M. Gerami[6], J.N. Gonçalves[3], H. Hofsäss[10], A. L. Kholkin[3], E. Kröll[2], A.A. Lourenço[3], D. C. Lupascu[2], R.P. Moreira[1], G.P. Oliveira[1], G. A. Cabrera-Pasca[12], P. Rocha-Rodrigues[1], T. S. N. Sales[4] , B. Bosch-Santos[11], S.S.M. Santos[1], E.L. Silva[1], M.R. Silva[3], R. N. Saxena[4], M. Schmück[2], V. Shvartsman[2], K. van Stiphout[10], A. Stroppa[7], P.B. Tavares[8], D. Zyabkin[9], P. Schaaf[9]

1 Institute of Physics for Advanced Materials, Nanotechnology and Photonics (IFIMUP), 4169 - 007 Porto
2 Institute for Materials Science and Center for Nanointegration Duisburg-Essen (CENIDE), Duisburg-Essen University, 45141 Essen
3 Centre for Research in Ceramics and Composite Materials, CICECO, Aveiro University, 3810-193 Aveiro
4 Instituto de Pesquisas Energéticas e Nucleares - IPEN, São Paulo
5 Centro de Ciências e Tecnologias Nucleares (C2TN) Instituto Superior Técnico, Lisbon University, Lisbon
6 European Organization for Nuclear Research (CERN), CH-1211 Geneva
7 SuPerconducting and other INnovative materials and devices institute (SPIN), 67100 L'Aquila
8 Centro de Química, Universidade de Trás-os-Montes e Alto Douro, 5000-801 Vila Real
9 Chair Materials for Electrical Engineering and Electronics, Institute of Materials Science and Engineering, Institute of Micro and Nanotechnologies MacroNano®, TU Ilmenau, 98693 Ilmenau
10 Fakultät für Physik, Universität Göttingen, Friedrich-Hund-PLatz 1, 37077 Göttingen
11 Material Measurement Laboratory, NIST, Gaithersburg, MD 20899
12 Universidade Federal do Pará (UFPA), Abaetetuba, Pará, Brazil

Spokesperson(s): A.M.L. Lopes (armandina.lopes@fc.up.pt) and Juliana Schell (juliana.schell@cern.ch)
Local contact: J. G. Correia (guilherme.correia@cern.ch)

Abstract

The proposal Probing Energy Efficient Perovskites (PEEP) aims to provide local and element selective information on the structural, electronic and magnetic properties, interactions and cross-coupling effects on perovskites, nowadays relevant for green technologies. Using Perturbed Angular Correlation (PAC) radioactive nuclear technique we intend to contribute to the understanding of the role of local landscapes, such as octahedra rotations, tilts and distortions, on the ferroic macroscopic orders. This project builds up from the previous experience in measuring magnetic hyperfine fields and electric field gradients on multiferroic materials to put forward a coordinated effort to study a set of archetypal ferroic structures. Herein we will complement our local probe studies with conventional macroscopic characterization techniques, symmetry analysis and first-principles simulations (DFT ab-initio) of the phase transitions occurring varying temperature or other external

stimulus. The use of appropriate PAC probe elements, such as the ^{111m}Cd/Cd, ^{204m}Pb/Pb and ^{204}Bi/Pb radioactive isotopes, specifically requires beams produced at ISOLDE.

Requested shifts: **17+17 shifts, (split into 4 runs over 2 years)**

1. Motivation

One of the most important challenges of this century is to find original strategies and materials to answer the societal and technological necessities that compel the development of novel sources of green energy and low power consumption electronics. Here, the rational control of ferroic orders through lattice distortions in perovskites and layered perovskites structures offers inspiring routes towards those requirements as unique magneto-electric or ferroelectric–photovoltaic effects are conspicuous in perovskites systems. In particular, the magnetization control by small electric pulses, using magneto-electric effect, anticipates a more energy efficient electronics world [1], [2]. On the other hand, ferroelectric-photovoltaics convert solar energy directly into electricity, where similar lattice distortions can well separate electron–hole pairs in ferroelectrics with small band gaps, being thus one of the dominant technologies for a green future [3], [4].

These and many other remarkable physical properties of ferroic/multiferroic materials arise from a spontaneous symmetry breaking. Below this point, these materials display a non-centrosymmetric structure and while for proper-ferroelectrics the polarization is the primary order parameter, driven by single zone-center polar lattice distortion, for improper-ferroelectrics, instead, the polarization is part of a more complex instability, that acts as the primary order parameter and allows for the breaking of inversion-symmetry. In general, these non-polar order parameters can have different physical origins and can be related to rotations or tilts of perovskite cages, magnetic or charge ordering [5], [6]. Also, a similar mechanism was observed in layered perovskites, where the lattice distortions that drive ferroelectricity are due to the coupling of non-polar rotations. This defines a more recent class of ferroelectrics, the Hybrid Improper - HIF ones, predicted in even-layered Ruddlesden-Popper materials [7].

Technological applicable multiferroic or ferroelectric-photovoltaics materials are rare and high-quality artificially ones are in general difficult and costly to produce. In this respect, the structural and compositional flexibility of perovskites and perovskite related structures might provide a direct impact to the mentioned technologies. However, to enhance the capabilities of such systems it is necessary to guide and tune the design for achieving maximum efficiencies. Thus, to accelerate the discovery of promising materials for sustainable energy solutions a joint effort of solid-state chemists, physicists, and ab-initio computer-simulation experts, with the exceptional ad-value of the use of nuclear radioactive techniques as Perturbed Angular Correlation (PAC), is put forward. Here, the local, nanoscopic probing via PAC, with its local selective electrical and magnetic output information, is a fundamental part of the process, as the lattice distortions, static or dynamic, at the origin of the functional properties, are sometimes not grasped by direct macroscopic signatures. Of particular interest is to understand how the individual modes evolve within a symmetry and also how they follow a chosen property, e.g. the polarization. In fact, it has been demonstrated that the polarization of RP compounds is determined by the combined effects of tilting and rotation modes [8] and not simply by the Goldschmidt tolerance factor [9]. This symmetry related fine details can be monitored via precise hyperfine measurements as we recently reported [10].

The PEEP alliance follows the collaborative research methodology of previous projects, such as IS390, IS487 and IS647, but the new working program, is strengthened by a discerning

symmetry analysis and first-principles simulations (using DFT- density functional methods such as VASP and Wien2k) with dedicated projects granted and running in the international PRACE supercomputing facility. The scientific topic and the diversified expertise of the team will provide a fertile ground for training new talented students in a highly international environment. Students and young researchers will master ab-initio simulations, material characterization, including nuclear techniques and/or theoretical aspects of multiferroic systems, according to their skills.

Following previous PAC studies in ferroelectric systems [5], [6], [10]–[14], here we propose to study the particularities of representative examples of the paradigmatic types of ferroelectricity in multiferroics which are known as i) hybrid improper ferroelectricity ii) proper ferroelectricity; ii) improper ferroelectricity. The specifics of the motivations and proposed studies of each system are presented below

2. CASE STUDIES

$Ca_{3-x}Sr_xTi_{2-y}Sn_yO_7$ Ruddlesden-Popper compounds - Naturally layered perovskites such as the Ruddlesden-Popper (RP) phases, with general formula $A_{n+1}B_nO3_{n+1}$ (A: rare earth or alkaline-earth and B: transition metal) are studied as feasible routes to develop novel functional materials [3]. Their structure consists of a series of stacked ABO_3 perovskite blocks intercalated with a rock-salt like AO layers. In particular, $Ca_3Mn_2O_7$ and $Ca_3Ti_2O_7$ compounds, were studied by Benedek *et al.* [7] through first-principles density functional theory (DFT), proposing them as a prototypical hybrid improper ferroelectrics (HIF). The HIF mechanism was confirmed in $Ca_3Ti_2O_7$, as well as in Sr-doped $Ca_3Ti_2O_7$ [15].

Above room temperature the $Ca_3(Mn,Ti)_2O_7$ crystal structure was predicted to be tetragonal-T, space group *I4/mmm*, and orthorhombic-O (*A21am*) at the lower temperature ferroelectric phase. Using PAC technique combined with ab-initio electronic structure calculations we confirmed those predictions by following the structural pathway that Ca3Mn2O7 takes from the low temperature O-polar phase to the high temperature tetragonal one, passing though the O´(Acaa) symmetry [10]. How the orthorhombic phase transforms into the undistorted prototype structure upon heating or upon cation site-selective isovalent substitutions has been the subject of many theoretical works[16]–[18]. Meanwhile, experimentally it has been verified that each compound [e.g. $(Sr,Ca)_3Ti_2O_7$ [19], [20] $(Sr,Ca)_3Sn_2O_7$ [9], $(Sr,Ca)_3Zr_2O_7$ [21] presents its unique path with direct impact on the magnetic and ferroelectric properties.

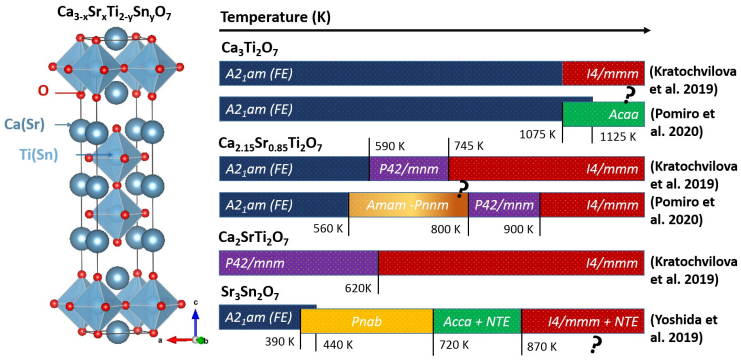

Fig 1. $Ca_{3-x}Sr_xTi_{2-y}Sn_yO_7$ structure and symmetries paths

In fact, while in $Ca_3Mn_2O_7$ an intermediate O´(*Acaa*) phase was observed [10], for $Ca_3Ti_2O_7$ and $(Sr_xCa_{1-x})_3Ti_2O_7$ (i.e. Ca-rich side), Pomiro el al. [19] reported that the structure transition proceeds directly from the polar O phase to the tetragonal *I4/mmm* (see fig. 1). On the other side, for the Sr-rich compositions, a different intermediate phase (*P42/mnm*) was reported [19]. More recently, $Ca_3Ti_2O_7$ was claimed to present a O-O´phase coexistence and a first-

order phase transition. For compositions with x~1 a gradual change in the octahedra rotation was reported to occur continuously with temperature, crossing five symmetries from the polar structure at room temperature to the undistorted tetragonal phase at high temperature (via P42/mnm), allowing for second-order phase transition. Both types of transitions can emerge in the intermediate compositions. This suggests the existence of a tri-critical point, where a first-order transition changes into a second-order one [19], a scenario worth exploring.
Similarly, we should expect an amazingly rich set of structure paths for $(Sr,Ca)_3Sn_2O_7$. The Sr end member was reported in 2017 as the first ferroelectric Sn insulator with switchable electric polarization [22] and already here a rich transition pathway was reported [9], [23]. Doubts arise however to whether the highest temperature phase is correctly indexed since our PAC and powder neutron diffraction results [24] in Ca2MnO4 showed that the *c* axis trend changes (positive to negative thermal expansion transition) concomitantly with the I4/mmm structural transition.

Here, we aim to resolve the conflicting symmetry models and unveil how the individual order parameters evolve and impact on ferroelectric properties. The focus will be placed on the - $Ca_{3-x}Sr_xTi_{2-y}Sn_yO_7$ end members and x=0.8 system. We propose to study this material using ^{111m}Cd/Cd, delivered in ppm concentrations, to probe the Ca/Sr site [10].

KNdTa2O7 Dion-Jacobson oxides - Hybrid improper ferroelectricity was also found in some $A'AB_2O_7$ Dion-Jacobson oxides, which like $Ca_3Mn_2O_7$, are also naturally layered perovskites, consisting also of a stack of perovskites layers, two octahedra thick, but intercalated with a distinct arrangement set of large A'-cations (A'= Cs or Rb) [25](Fig.1). By substituting the A' cation ions in systems as in $A'NdB_2O_7$, (B= Nb, Ta), several structural factors can be tuned modifying consequently the relative overlapping of adjacent perovskite blocks, and also the degree of octahedra tilting and rotation within the perovskite layers, Fig.2.

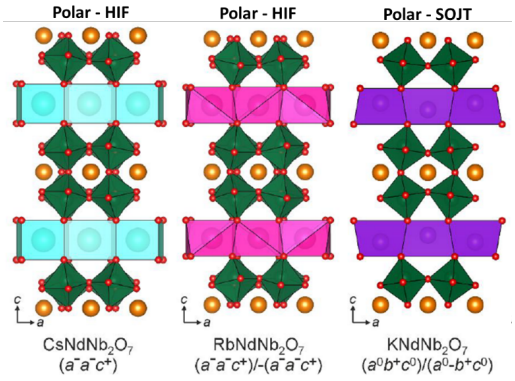

Fig. 2. Naturally layered perovskite $A'NdNb_2O_7$ upon cation-exchange (from [26]).

The $KNdNb_2O_7$ and $KNdTa_2O_7$ compounds have proven also to adopt polar structures, however unlike in $CsNdM_2O_7$ and $RbNdM_2O_7$ (M = Nb, Ta) or the R.P. systems $Ca_3Mn_2O_7$ or $Ca_3Ti_2O_7$, where the polar structure arises from the condensation of two octahedra rotation modes via the hybrid improper ferroelectric coupling mechanism, the $KNdNb_2O_7$ and $KNdTa_2O_7$ structures are suggested to present the *Im2m* symmetry, with a single octahedral rotation mode [26]. Here the polar nature is attributed to a second-order Jahn-Teller (SOJT) distortion of the NbO_6/TaO_6 units, where the Nb and Ta cations are significantly displaced from the respective octahedra centres [26].

We thus aim to perform a comparative local study within these two different polar natures upon Cs or K substitution. The focus will be placed on the – $Cs(K)NdTa_2O_7$ system. We propose to study this material using ^{111m}Cd/Cd and ^{181}Hf/^{181}Ta in order to investigate local properties at the A and B sites, respectively.

$PbFe_{2/3}W_{1/3}O_3$ Perovskite - A common mechanism in perovskite ferroelectrics lies in collective ionic displacements of electronic origin driven by off-centering of the A cation, via the second-order Jahn-Teller (SOJT) effect. This effect is favourable for d^0 or $6s^2$ cations such as Pb^{2+} and Bi^{3+} and might be at the origin of the dielectric properties of $PbFe_{2/3}W_{1/3}O_3$ (PFW). This compound belongs to single phase type-I multiferroics [27], where the ferroelectric and magnetic ordering are related to A-site (Pb^{2+}) and B-site (Fe^{3+}) cations, respectively. Contrary to most of the single phase multiferroics, the transition into magnetic ordered state occurs in PFW at much higher temperatures (paramagnetic-to-antiferromagnetic T_N lies in the range of 350–380 K) than the ferroelectric phase transition (T_c ~150–200 K) [28]. This makes PFW especially interesting from the point of view of coupling between magnetic and polar degrees of freedom. Several conventional techniques have been applied to study this material, however limited progress has been achieved due to its complex magnetic structure [29]. A second transition at T_{N2} ~20 K has been observed [30], the nature of which is still a matter of discussion.

PAC measurements can be carried out in the temperature range covering all the transitions (see fig 3) and deliver valuable information about the evolution of the structure, the ferroic orders, and magnetoelectric coupling of the material. More specifically, the PAC technique can help to understand the origin of the anomaly in the lattice parameters variation [28], investigate the origin of the weak magnetoelectric coupling interaction and the variation of magnetic susceptibility at T_C [29].

Here we propose to study this material using ^{111m}Cd, ^{204m}Pb and ^{204}Bi in order to investigate local properties at the A and B sites.

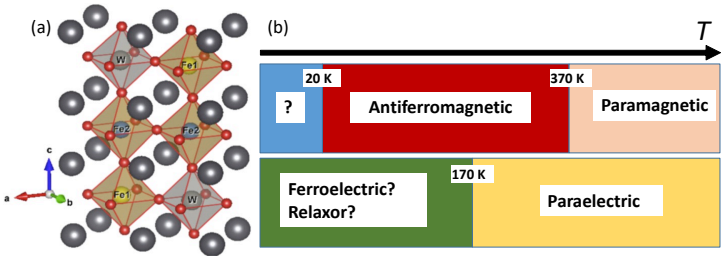

(a) Ground state geometry of PFW lattice [28]. (b) Sequence of the phase transition in PFW.

Double perovskites - with the chemical formula La_2TMnO_6, where T is a transition metal, such as Ti, V, Cr, Fe, Co or Ni [31], has attracted attention particularly due to their rare ferromagnetic-dielectric behavior close to room temperature, which opens up the possibility of technological applications [32]. The relatively high temperatures of the ferromagnetic ordering are dependent on the ordering of the cationic spins on the B site (T^{2+} and Mn^{4+}) and on the superexchange interaction in T-O-Mn, generally forming an angle of 180° via oxygen atoms. In this structure, the spins of the T^{2+} atoms (with orbitals e_g semi-filled) and Mn^{4+} (with orbitals e_g empty) interact by the superexchange interaction via adjacent oxygen atoms following the rules of Goodenough-Kanamori which predict relatively high Curie temperatures [33], [34]. This is the case of La_2NiMnO_6 that although not presenting a polar order, its ferromagnetic ordering occurs at T_C = 280 K, very close to room temperature [35], [36]. This compound nanoparticles however, showed a ferromagnetic ordering at 196 K [37]. The structure of La_2NiMnO_6 is rhombohedral ($R\bar{3}$) at high temperatures and becomes monoclinic ($P2_1/n$) at low temperatures, both coexisting over a wide temperature range [35]. La_2CoMnO_6, on the other hand, crystallizes in the monoclinic structure P121/n1 presenting ferromagnetic ordering with T_C = 230 K and a high saturation magnetization M_S = 6 μ_B /f. u. [38], [39]. This high ferromagnetic ordering temperature is due to the highly ordered arrangement of Co^{2+} and Mn^{4+} atoms in the perovskite B sites, while a disordered arrangement of Co^{3+} and Mn^{3+} atoms in the B sites contributes to a lower Curie temperature [40].

Quite different properties, comparing with the former oxides, are exhibited by La_2CrMnO_6. Experimental measurements show conflicting results regarding structural, magnetic and electronic behavior.
The mixed perovskite La(Cr,Mn)O3 present monoclinic structure [41], whereas La2CrMnO6 has been reported to be rhombohedral with ferromagnetic ordering at 190 K [42] and orthorhombic with P*bnm* symmetry and ferromagnetic ordering through the Griffiths-like phase at 180 K and spin-glass transitions at 4.7 K and 107.8 K [43]. Another study reports orthorhombic structure with ferrimagnetic ordering at 118 K [44]. Additionally, thin films of La_2CrMnO_6 have been reported to crystallize in the orthorhombic structure with structural order and ferrimagnetism at low temperature (100 K) [45].

Here, we aim to investigate, focusing in La_2TMnO_6 (T = Cr, Ni, Co), the role of local distortions in the ferroelectric properties and the influence of the transition metal and the T-Mn disorder on the magnetic behavior. We propose to study these DP using ^{111m}Cd to probe the La site [46] of the perovskites. Complementary measurements using ^{140}La(^{140}Ce) probe, very sensitive to magnetic hyperfine interactions, will be performed IPEN, São Paulo. Preliminary PAC results using ^{111m}Cd in $LaBaMn_2O_6$ double perovskite are published in [47].

Summary of requested shifts:

The work plan assigns one specific case study to each team of experts of the PEEP collaboration. The complementarity of the systems allows, through collaborative work and efficient use of equipment and resources, to obtain an integrated view of the role of local distortions upon tuning ferroic properties. All samples will be synthesized and macroscopically characterized in the PEEP partner institutes.

ISOLDE Beam	Intensity (ion/μC of p-beam)	Target	Ion source	SHIFTS per year	Systems
^{111m}Cd (48 m)	1. 10^8	Molten Sn	Vadis	2+2	$Ca_{3-x}Sr_xTi_{2-y}Sn_yO_7$
				2+2	$Cs(K)NdTa_2O_7$
			MK5	1+1	$PbFe_{2/3}W_{1/3}O_3$
				2+2	$La_2(Cr, Co, Ni)MnO_6$
^{204m}Pb (67m)	5 . 10^7	UC2	RILIS	2	$PbFe_{2/3}W_{1/3}O_3$
^{204}Bi (11.2h)	1 . 10^7	UC2	RILIS	1	$PbFe_{2/3}W_{1/3}O_3$

^{111m}Cd/Cd – is the main probe isotope required to achieve the PEEP aims, considering that it has been previously successfully used and tested in most compounds under study, to occupy the PK A cation site(s). Willing to explore the B site(s) we consider experimental campaigns using ^{111}In/Cd($t_{1/2}$ =2.8d) or ^{181}Hf/^{181}Ta($t_{1/2}$ =45d) with the help of the ISKP Bonn implanter. ^{204}Bi/Pb and ^{204m}Pb/Pb: The ^{204m}Pb/Pb short lived probe case is similar – on beam time, sample preparation and measurement requirements to ^{111m}Cd. Both Bi and Pb isotopes are ideal probes for Bi and Pb compounds and ideally delivered separately. Experiments using ^{204}Bi/Pb will profit from the use of digital setups with LaBr3 scintillators that separate γ_1 (912 keV) of ^{204m}Pb (~14%) from γ_1 (984 keV) (~59%) after ^{204}Bi decay, one unique way to identify if delayed electronic recombination will be observable after ^{204}Bi decay [47].

References:

[1] R. Ramesh and N. A. Spaldin, “Multiferroics: progress and prospects in thin films,” *Nat. Mater.*, vol. 6, no. 1, pp. 21–29, 2007, doi: 10.1038/nmat1805

[2] M. Bibes and A. Barthélémy, “Multiferroics: Towards a magnetoelectric memory,” *Nat. Mater.*, vol. 7, no. 6, pp. 425–426, 2008, doi: 10.1038/nmat2189

[3] H. Wang, G. Gou, and J. Li, “Ruddlesden-Popper perovskite sulfides A3B2S7: A new family of ferroelectric photovoltaic materials for the visible spectrum,” *Nano Energy*, vol. 22, pp. 507–513, Apr. 2016, doi: 10.1016/j.nanoen.2016.02.036

[4] I. E. Castelli, T. Olsen, and Y. Chen, “Towards photoferroic materials by design: recent progress and perspectives,” *J. Phys. Energy*, vol. 2, no. 1, p. 011001, Nov. 2019, doi: 10.1088/2515-7655/ab428c

[5] A. M. L. Lopes, J. P. Araújo, V. S. Amaral, J. G. Correia, Y. Tomioka, and Y. Tokura, “New phase transition in the Pr1-xCaxMnO3 system: Evidence for electrical polarization in charge ordered manganites,” *Phys. Rev. Lett.*, vol. 100, no. 15, p. 155702, Apr. 2008, doi: 10.1103/PhysRevLett.100.155702

[6] G. N. P. Oliveira, R. C. Teixeira, R. P. Moreira, J. G. Correia, J. P. Araújo, and A. M. L. Lopes, “Local inhomogeneous state in multiferroic SmCrO3,” *Sci. Rep.*, vol. 10, no. 1, pp. 1–12, Dec. 2020, doi: 10.1038/s41598-020-61384-6

[7] N. A. Benedek and C. J. Fennie, “Hybrid improper ferroelectricity: A mechanism for controllable polarization-magnetization coupling,” *Phys. Rev. Lett.*, vol. 106, no. 10, p. 107204, Mar. 2011, doi: 10.1103/PhysRevLett.106.107204

[8] B. H. Chen, T. L. Sun, X. Q. Liu, X. L. Zhu, H. Tian, and X. M. Chen, “Enhanced hybrid improper ferroelectricity in Sr3-xBaxSn2O7 ceramics with a Ruddlesden-Popper (R-P) structure,” *Appl. Phys. Lett.*, vol. 116, no. 4, p. 042903, Jan. 2020, doi: 10.1063/1.5138672

[9] S. Yoshida *et al.*, “Hybrid Improper Ferroelectricity in (Sr,Ca)3Sn2O7 and Beyond: Universal Relationship between Ferroelectric Transition Temperature and Tolerance Factor in n = 2 Ruddlesden-Popper Phases,” *J. Am. Chem. Soc.*, vol. 140, no. 46, pp. 15690–15700, Nov. 2018, doi: 10.1021/jacs.8b07998

[10] P. Rocha-Rodrigues *et al.*, “Ca3Mn2 O7 structural path unraveled by atomic-scale properties: A combined experimental and ab initio study,” *Phys. Rev. B*, vol. 101, no. 6, p. 64103, Feb. 2020, doi: 10.1103/PhysRevB.101.064103

[11] G. N. P. Oliveira *et al.*, “Dynamic off-centering of Cr3+ ions and short-range magneto-electric clusters in CdCr2S4,” *Phys. Rev. B - Condens. Matter Mater. Phys.*, vol. 86, no. 22, p. 224418, Dec. 2012, doi: 10.1103/PhysRevB.86.224418

[12] J. N. Gonçalves *et al.*, “Ab initio study of the relation between electric polarization and electric field gradients in ferroelectrics,” *Phys. Rev. B - Condens. Matter Mater. Phys.*, vol. 86, no. 3, p. 035145, Jul. 2012, doi: 10.1103/PhysRevB.86.035145

[13] A. M. L. Lopes *et al.*, “Local distortions in multiferroic AgCrO2 triangular spin lattice,” *Phys. Rev. B - Condens. Matter Mater. Phys.*, vol. 84, no. 1, p. 014434, Jul. 2011, doi: 10.1103/PhysRevB.84.014434

[14] J. Schell, H. Hofsäss, and D. C. Lupascu, “Using radioactive beams to unravel local phenomena in ferroic and multiferroic materials,” *Nucl. Instruments Methods Phys. Res. Sect. B Beam Interact.*

with Mater. Atoms, vol. 463, pp. 134–137, Jan. 2020, doi: 10.1016/j.nimb.2019.06.016

[15] Y. S. Oh, X. Luo, F. T. Huang, Y. Wang, and S. W. Cheong, "Experimental demonstration of hybrid improper ferroelectricity and the presence of abundant charged walls in (Ca,Sr)3Ti2O7 crystals," *Nat. Mater.*, vol. 14, no. 4, pp. 407–413, 2015, doi: 10.1038/nmat4168

[16] A. B. Harris, "Symmetry analysis for the Ruddlesden-Popper systems Ca3Mn 2O7 and Ca3Ti2O7," *Phys. Rev. B - Condens. Matter Mater. Phys.*, vol. 84, no. 6, p. 064116, Aug. 2011, doi: 10.1103/PhysRevB.84.064116

[17] N. A. Benedek, J. M. Rondinelli, H. Djani, P. Ghosez, and P. Lightfoot, "Understanding ferroelectricity in layered perovskites: New ideas and insights from theory and experiments," *Dalt. Trans.*, vol. 44, no. 23, pp. 10543–10558, Jun. 2015, doi: 10.1039/c5dt00010f

[18] C. F. Li *et al.*, "Structural transitions in hybrid improper ferroelectric C a3 T i2 O7 tuned by site-selective isovalent substitutions: A first-principles study," *Phys. Rev. B*, vol. 97, no. 18, p. 184105, May 2018, doi: 10.1103/PhysRevB.97.184105

[19] M. Kratochvilova *et al.*, "Mapping the structural transitions controlled by the trilinear coupling in Ca3- xSr x Ti2O7," *J. Appl. Phys.*, vol. 125, no. 24, p. 244102, Jun. 2019, doi: 10.1063/1.5089723

[20] F. Pomiro *et al.*, "From first- To second-order phase transitions in hybrid improper ferroelectrics through entropy stabilization," *Phys. Rev. B*, vol. 102, no. 1, p. 14101, Jul. 2020, doi: 10.1103/PhysRevB.102.014101

[21] S. Yoshida *et al.*, "Ferroelectric $Sr_3Zr_2O_7$: Competition between Hybrid Improper Ferroelectric and Antiferroelectric Mechanisms," *Adv. Funct. Mater.*, vol. 28, no. 30, p. 1801856, Jul. 2018, doi: 10.1002/adfm.201801856

[22] Y. Wang, F.-T. Huang, X. Luo, B. Gao, and S.-W. Cheong, "The First Room-Temperature Ferroelectric Sn Insulator and Its Polarization Switching Kinetics," *Adv. Mater.*, vol. 29, no. 2, p. 1601288, Jan. 2017, doi: 10.1002/adma.201601288

[23] X. Xu, Y. Wang, F. Huang, K. Du, E. A. Nowadnick, and S. Cheong, "Highly Tunable Ferroelectricity in Hybrid Improper Ferroelectric $Sr_3Sn_2O_7$," *Adv. Funct. Mater.*, p. 2003623, Aug. 2020, doi: 10.1002/adfm.202003623

[24] P. Rocha-Rodrigues *et al.*, "Physical Review B - Accepted Paper: Ca_2MnO_4 structural path: Following the negative thermal expansion at the local scale," Accessed: Sep. 21, 2020. [Online]. Available: https://journals.aps.org/prb/accepted/d207eO3aF991b937a98066857e7c22ee46c01b4f5

[25] T. Zhu, A. S. Gibbs, N. A. Benedek, and M. A. Hayward, "Complex Structural Phase Transitions of the Hybrid Improper Polar Dion-Jacobson Oxides RbNdM2O7 and CsNdM2O7 (M = Nb, Ta)," *Chem. Mater.*, vol. 32, no. 10, pp. 4340–4346, May 2020, doi: 10.1021/acs.chemmater.0c01304

[26] S. Mallick, A. S. Gibbs, W. Zhang, P. S. Halasyamani, N. A. Benedek, and M. A. Hayward, "The Polar Structures of KNdNb2O7 and KNdTa2O7.," *Chem. Mater.*, vol. 11, p. acs.chemmater.0c02846, 2020, doi: 10.1021/acs.chemmater.0c02846

[27] D. Khomskii, "Classifying multiferroics: Mechanisms and effects," *Physics (College. Park. Md).*, vol. 2, p. 20, 2009, doi: 10.1103/Physics.2.20

[28] S. A. Ivanov, S. G. Eriksson, R. Tellgren, and H. Rundlöf, "Neutron powder diffraction study of the magnetoelectric relaxor Pb(Fe 2/3W1/3)O3," *Mater. Res. Bull.*, vol. 39, no. 14–15, pp. 2317–2328, Dec. 2004, doi: 10.1016/j.materresbull.2004.07.025

[29] I. Shivaraja, S. Matteppanavar, S. Rayaprol, and B. Angadi, "Evidence of weak ferromagnetic and antiferromagnetic interaction at low temperature in Pb(Fe2/3W1/3)O3 multiferroic," *Phys. B*

Condens. Matter, vol. 561, pp. 114–120, May 2019, doi: 10.1016/j.physb.2019.02.062

[30] Z.-G. Ye, K. Toda, M. Sato, E. Kita, and H. Schmid, "Synthesis, structure and properties of the magnetic relaxor ferroelectric Pb(Fe2/3W1/3)O3," *J. Korean Phys. Soc.*, vol. 32, pp. S1028–S1031, 1998, Available: https://archive-ouverte.unige.ch/unige:31129

[31] H. Chen and A. Millis, "Antisite defects at oxide interfaces," *Phys. Rev. B*, vol. 93, no. 10, p. 104111, Mar. 2016, doi: 10.1103/PhysRevB.93.104111

[32] H. J. Zhao, W. Ren, Y. Yang, J. Íñiguez, X. M. Chen, and L. Bellaiche, "Near room-temperature multiferroic materials with tunable ferromagnetic and electrical properties," *Nat. Commun.*, vol. 5, no. 1, pp. 1–7, May 2014, doi: 10.1038/ncomms5021

[33] J. B. Goodenough, "Theory of the role of covalence in the perovskite-type manganites [La,M(II)]MnO3," *Phys. Rev.*, vol. 100, no. 2, pp. 564–573, Oct. 1955, doi: 10.1103/PhysRev.100.564

[34] J. Kanamori, "Superexchange interaction and symmetry properties of electron orbitals," *J. Phys. Chem. Solids*, vol. 10, no. 2–3, pp. 87–98, Jul. 1959, doi: 10.1016/0022-3697(59)90061-7

[35] I. Dass, J. Q. Yan, and B. Goodenough, "Oxygen stoichiometry, ferromagnetism, and transport properties of La2-xNiMnO6+δ," *Phys. Rev. B - Condens. Matter Mater. Phys.*, vol. 68, no. 6, p. 064415, Aug. 2003, doi: 10.1103/PhysRevB.68.064415

[36] N. S. Rogado, J. Li, A. W. Sleight, and M. A. Subramanian, "Magnetocapacitance and magnetoresistance near room temperature in a ferromagnetic semiconductor: La2NiMnO6," *Adv. Mater.*, vol. 17, no. 18, pp. 2225–2227, Sep. 2005, doi: 10.1002/adma.200500737

[37] M. G. Masud, A. Ghosh, J. Sannigrahi, and B. K. Chaudhuri, "Observation of relaxor ferroelectricity and multiferroic behaviour in nanoparticles of the ferromagnetic semiconductor La 2NiMnO 6," *J. Phys. Condens. Matter*, vol. 24, no. 29, Jul. 2012, doi: 10.1088/0953-8984/24/29/295902

[38] R. I. Dass and J. B. Goodenough, "Multiple magnetic phases of $La_2CoMnO_{6-\delta}$ (0 <~ δ <~ 0 . 0 5)," *Phys. Rev. B - Condens. Matter Mater. Phys.*, vol. 67, no. 1, p. 014401, Jan. 2003, doi: 10.1103/PhysRevB.67.014401

[39] R. Egoavil *et al.*, "Phase problem in the B-site ordering of La2CoMnO6: Impact on structure and magnetism," *Nanoscale*, vol. 7, no. 21, pp. 9835–9843, Jun. 2015, doi: 10.1039/c5nr01642h

[40] Y. Q. Lin and X. M. Chen, "Dielectric, Ferromagnetic Characteristics, and Room-Temperature Magnetodielectric Effects in Double Perovskite La2CoMnO6 Ceramics," *J. Am. Ceram. Soc.*, vol. 94, no. 3, pp. 782–787, Mar. 2011, doi: 10.1111/j.1551-2916.2010.04139.x

[41] U. H. Bents, "Neutron Diffraction Study of the Magnetic Structures for the Perovskite-Type Mixed Oxides la (Mn, Cr)O3," *Phys. Rev.*, vol. 106, no. 2, pp. 225–230, Apr. 1957, doi: 10.1103/PhysRev.106.225

[42] P. Barrozo and J. Albino Aguiar, "Ferromagnetism in Mn half-doped LaCrO3 perovskite," in *Journal of Applied Physics*, May 2013, vol. 113, no. 17, p. 17E309, doi: 10.1063/1.4801507

[43] J. P. Palakkal, C. Raj Sankar, and M. R. Varma, "Multiple magnetic transitions, Griffiths-like phase, and magnetoresistance in La2CrMnO6," *J. Appl. Phys.*, vol. 122, no. 7, p. 073907, Aug. 2017, doi: 10.1063/1.4999031

[44] D. Yang, P. Zhao, S. Huang, T. Yang, and D. Huo, "Ferrimagnetism, resistivity, and magnetic exchange interactions in double perovskite La2CrMnO6," *Results Phys.*, vol. 12, pp. 344–348, Mar. 2019, doi: 10.1016/j.rinp.2018.11.090

[45] K. Yoshimatsu *et al.*, "Magnetic and electronic properties of B -site-ordered double-perovskite

oxide L a2CrMn O6 thin films," *Phys. Rev. B*, vol. 99, no. 23, p. 235129, Jun. 2019, doi: 10.1103/PhysRevB.99.235129

[46] A. M. L. Lopes, J. P. Araújo, J. J. Ramasco, V. S. Amaral, R. Suryanarayanan, and J. G. Correia, "Percolative transition on ferromagnetic insulator manganites: Uncorrelated to correlated polaron clusters," *Phys. Rev. B*, vol. 73, no. 10, Mar. 2006, doi: 10.1103/physrevb.73.100408

[47] B. Bosch-Santos *et al.*, "Magnetic field at Ce impurities in la sites of $La_{0.5}Ba_{0.5}MnO_3$ double perovskites," *AIP Adv.*, vol. 9, no. 3, p. 035245, Mar. 2019, doi: 10.1063/1.5080094

[48] M. Nagl, U. Vetter, M. Uhrmacher, and H. Hofsäss, "A new all-digital time differential γ-γ Angular correlation spectrometer," *Rev. Sci. Instrum.*, vol. 81, no. 7, p. 073501, Jul. 2010, doi: 10.1063/1.3455186

Appendix

DESCRIPTION OF THE PROPOSED EXPERIMENT

The experimental setup comprises: *(name the fixed-ISOLDE installations, as well as flexible elements of the experiment)*

Part of the Choose an item.	Availability	Design and manufacturing
SSP-chamber @ GLM	☒ Existing	☒ To be used without any modification
Existing equipment on the solid state labs in building 115 or 508-R-002, R-004 and R-008 - PAC analogue and digital detector setups - annealing and measurement furnaces, closed cycle refrigerators, chillers, LN2 dewars (0.5, 1, 2, 3 liter containers)	☒ Existing	☐ To be used without any modification ☐ To be modified
	☐ New	☐ Standard equipment supplied by a manufacturer ☐ CERN/collaboration responsible for the design and/or manufacturing
[Part 2 experiment/ equipment]	☐ Existing	☐ To be used without any modification ☐ To be modified
	☐ New	☐ Standard equipment supplied by a manufacturer ☐ CERN/collaboration responsible for the design and/or manufacturing
[insert lines if needed]		

HAZARDS GENERATED BY THE EXPERIMENT

Hazards named in the document relevant for the fixed SSP-GLM chamber and building 508 installations.

Additional hazards:

Hazards			
	SSP-GLM	*Building 508-R-04,08*	*[Part 3 of the experiment/equipment]*
Thermodynamic and fluidic			
Pressure	[pressure][Bar], [volume][l]		

Vacuum	10-6 mbar at SSP chamber 10 during collections		
Temperature	[temperature] [K]	temperature range of measurements and annealings [22ºC – 1000 ºC]	
Heat transfer			
Thermal properties of materials			
Cryogenic fluid	[fluid], [pressure][Bar], [volume][l]	Liquid nitrogen, 1 Bar, few litres used during the PAC measurements on appropriate dewars.	
Electrical and electromagnetic			
Electricity	[voltage] [V], [current][A]		
Static electricity			
Magnetic field	[magnetic field] [T]		
Batteries	☐		
Capacitors	☐		
Ionizing radiation			
Target material	[material]		
Beam particle type (e, p, ions, etc)	111mCd (49 m) 204mPb (67m) 204Bi (11.2h)		
Beam intensity			
Beam energy	50 keV		
Cooling liquids	[liquid]		
Gases	[gas]		
Calibration sources:	☐		
• Open source	☐ Produced at ISOLDE: 111mCd (48 m) 204mPb (67m) 204Bi (11.2h)	Sources to be manipulated at 508-r-002, 004 and measured at 508 - r- 008	
• Sealed source	☐ [ISO standard]	22Na, 60Co, 133Ba sources provided by RP services at CERN, used at 508	
• Isotope			
• Activity			
Use of activated material:			
• Description	☐		
• Dose rate on contact and in 10 cm distance	[dose][mSV]		
• Isotope			
• Activity	111mCd (49 m) < 15 MBq 204mPb (67m) < 5 MBq 204Bi (11.2h) < 3 MBq		
Non-ionizing radiation			
Laser			
UV light			
Microwaves (300MHz-30 GHz)			
Radiofrequency (1-300MHz)			
Chemical			
Toxic	[chemical agent], [quantity]		
Harmful	[chemical agent], [quantity]		

CMR (carcinogens, mutagens and substances toxic to reproduction)	[chemical agent], [quantity]		
Corrosive	[chemical agent], [quantity]		
Irritant	[chemical agent], [quantity]		
Flammable	[chemical agent], [quantity]		
Oxidizing	[chemical agent], [quantity]		
Explosiveness	[chemical agent], [quantity]		
Asphyxiant	[chemical agent], [quantity]		
Dangerous for the environment	[chemical agent], [quantity]		
Mechanical			
Physical impact or mechanical energy (moving parts)	[location]		
Mechanical properties (Sharp, rough, slippery)	[location]		
Vibration	[location]		
Vehicles and Means of Transport	[location]		
Noise			
Frequency	[frequency],[Hz] Ambient noise at the ISOLDE Hall, building 170		
Intensity	Ambient noise at the ISOLDE Hall, building 170		
Physical			
Confined spaces	[location]		
High workplaces	[location]		
Access to high workplaces	[location]		
Obstructions in passageways	[location]		
Manual handling	[location] All samples and sample holders are manually handled either by long tweezers to insert and extract the sample holder into and out of the SSP implantation chamber at GLM. Transportation of sample holders in between the SSP chamber and the fume hood on b.170 are done inside a metallic container. In the fume hood the samples are removed (about 3 per implantation batch) and closed on individual bags, or eppendorfs and merged inside led pots to be transported to b.508 r-002 and r-004	Once the individual samples arrive to b.508-r-002, r-004 these are further manipulated with tweezers on dedicated spaces to be controlled and annealed in the dedicated furnaces, or, optionally, already placed in special quartz containers and taken to b.508-r-008 to be measured at the PAC setups.	
Poor ergonomics	[location]		

0.1 Hazard identification

3.2 Average electrical power requirements (excluding fixed ISOLDE-installation mentioned above):
There is no additional equipment with relevant power consumption on these small-scale experiments.